Structural and magnetic properties of $DyMn_2D_6$ synthesized under high deuterium pressure

2009 J. Phys.: Condens. Matter 21 016001

(http://iopscience.iop.org/0953-8984/21/1/016001)

J. Phys.: Condens. Matter **21** (2009) 016001 (6pp) doi:10.1088/0953-8984/21/1/016001

Structural and magnetic properties of $DyMn_2D_6$ synthesized under high deuterium pressure

V Paul-Boncour[1,5], S M Filipek[2], R Wierzbicki[2], G André[3], F Bourée[3] and M Guillot[4]

[1] Laboratoire de Chimie Métallurgique des Terres Rares, CNRS, 2–8 rue H Dunant, 94320 Thiais, France
[2] Institute of Physical Chemistry, PAS, Ul. Kasprzaka 44/52, 01224 Warsaw, Poland
[3] Laboratoire Léon Brillouin, CEA-CNRS, CEA/Saclay, 91191 Gif-sur-Yvette, France
[4] LCMI, CNRS-MPI, BP166, 38042 Grenoble Cedex 9, France

E-mail: paulbon@glvt-cnrs.fr

Received 9 September 2008, in final form 24 October 2008
Published 1 December 2008
Online at stacks.iop.org/JPhysCM/21/016001

Abstract

$DyMn_2D_6$ has been prepared by applying high gaseous deuterium pressure on $DyMn_2$. This phase is isostructural with other RMn_2D_6 (R = Y, Er) compounds and crystallizes with a K_2PtCl_6 type structure having an ordered anion and a partially disordered cation arrangement because Dy and half the Mn atoms are randomly substituted in the same 8c site. The reverse susceptibility follows a Curie–Weiss law with an effective moment of 10 μ_B similar to that of $DyMn_2$. Short range magnetic order, corresponding to ferromagnetic correlations, is observed in the neutron patterns up to 10 K and can be attributed to Dy–Dy interactions. The decomposition of the deuteride into Mn and DyD_2, studied by thermal gravimetric analysis, occurs between 470 and 650 K. A further deuterium desorption takes place above 920 K.

1. Introduction

The application of high hydrogen or deuterium pressure on intermetallic compounds resulted in synthesis of a number of new metal hydrides/deuteride, in particular from Laves phase compounds. This has allowed the formation of $ZrCo_2H_2$ and $ZrFe_2H_4$, which keep the same C15 cubic structure as their parent compounds, and YFe_2H_5 and $ErFe_2H_5$, which display an orthorhombic distortion derived from the C15 structure [1, 2]. More surprising results have been obtained for RMn_2D_6 compounds with R = Y and Er, which crystallize in a new type of cubic structure having no relationship with the C15 or C14 structures of the pristine compounds [3, 4]. According to x-ray (XRD) and neutron powder diffraction (NPD) experiments, these RMn_2D_6 crystallize in a disordered fluorite structure (K_2PtCl_6 type). This structure can be described in the $Fm3m$ space group where the R and half of the Mn atoms (Mn1) occupy randomly the 8c site whereas the remaining Mn atoms (Mn2) are located in the 4a site being surrounded by six H atoms in the 24e site [3]. This is very different from that observed for the other RMn_2H_x hydrides (deuterides) ($0 < x \leqslant 4.5$), the structure of which is derived from the C15 or C14 structure. As a matter of fact, the crystal structure of YMn_2H_6 and $ErMn_2H_6$ results from a complete reorganization of the unit cell of the parent compound. YMn_2D_6 is a paramagnet which follows a modified Curie–Weiss law. NPD study from 1.5 to 290 K has confirmed the absence of long range magnetic order in YMn_2D_6. $ErMn_2D_6$ has a ferromagnetic behaviour, but NPD indicates only ferro- and antiferromagnetic short range order at low temperature.

The purpose of this work was to extend this study to other RMn_2 compounds in order to determine whether similar crystallographic and magnetic behaviour could be obtained. In this study we will present the results obtained for $DyMn_2D_6$, in particular its structural and magnetic properties using XRD and NPD experiments as well as magnetic measurements. The thermal deuterium desorption of this phase was also studied using thermal gravimetric analysis (TGA).

[5] Author to whom any correspondence should be addressed.

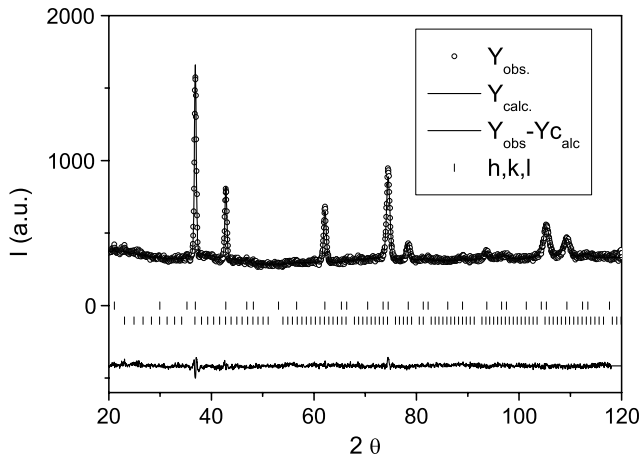

Figure 1. Experimental and refined NPD pattern of $DyMn_2D_6$ measured at 300 K on 3T2. The background slope is of instrumental origin. The upper *hkl* ticks correspond to the K_2PtCl_6 type structure, whereas the lower ones are related to DyO_2.

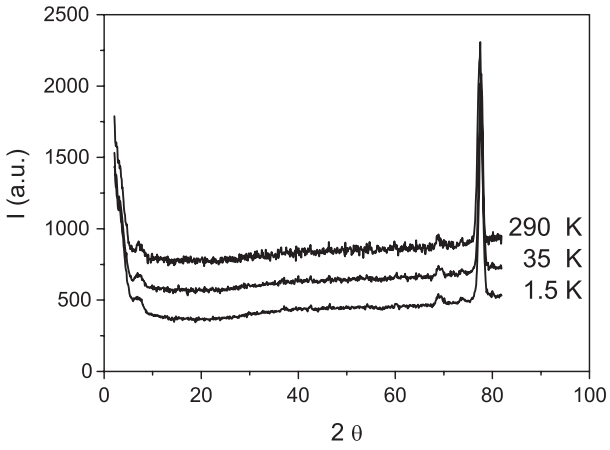

Figure 2. Experimental NPD patterns of $DyMn_2D_6$ measured on G4.1 at 1.5, 35 and 290 K.

These new results will be presented and discussed in relation to the structural and magnetic properties of the parent compound $DyMn_2$ and other RMn_2D_6 compounds.

2. Experimental details

$DyMn_2$ was prepared by induction melting of the pure elements (Dy 99.9% and Mn 99.99%) followed by an annealing treatment for 11 days at 1073 K. The homogeneity of the sample was checked by XRD and electron probe microanalysis (EPMA).

Initially the syntheses of RMn_2H_6 (R = Y, Er) were carried out at moderate pressures (50–200 MPa) of hydrogen at temperatures of about 550 K. However, at these conditions the syntheses were often unsuccessful (the sample decomposed into RH_x and metallic Mn). After some trial and error we found that the most appropriate conditions for reproducible synthesis of RMn_2H_6 and derivative compounds were 1 MPa (H_2) and 100 °C. The syntheses of $DyMn_2D_6$ (about 4 g) for the NPD experiments were carried out mainly under these conditions.

The XRD patterns were measured with a D8 Brucker diffractometer equipped with a rear graphite monochromator in the range $10° < 2\theta < 120°$ with a step of 0.02° using Cu Kα radiation. The NPD patterns of the deuteride were registered at 290 K on the 3T2 diffractometer and at temperatures varying between 1.5 and 290 K on the G4.1 diffractometer at the Laboratoire Léon Brillouin (LLB), Saclay. For the 3T2 experiment the wavelength was 1.225 Å and the angular range $6° < 2\theta < 125°$ with a step of 0.05°. For the G4.1 experiments the wavelength was 2.427 Å and the angular range was $2° < 2\theta < 82°$ with a step of 0.1°. The deuteride was contained in a vanadium sample holder. All the XRD and NPD patterns were refined with the Rietveld method, using the Fullprof code [5]. The line shapes were refined with a Pearson VII function.

The magnetic measurements in both AC and DC modes were performed using a Quantum Design physical properties measurement system (PPMS) operating up to 9 T. Additional magnetization measurements were performed with a magnetometer at the High Magnetic Field Laboratory, Grenoble, France, operating up to 23 T.

TGA was performed on a Setsys Evolution 1750 balance from Setaram operating from 300 to 1500 K. The powder was placed in an open Pt crucible and the experiment was performed with an Ar flow of 20 ml min^{-1}. The temperature was raised at a rate of 10 K min^{-1}.

3. Results

3.1. X-ray and neutron diffraction

The starting $DyMn_2$ compound contained 90% C15 phase with $a = 7.5895(3)$ Å and 10% C14 phase with $a = 5.3643(9)$ Å and $c = 8.7358(14)$ Å. After deuterium absorption at high pressure ($T = 280$ °C, $P = 0.05$ GPa or $T = 100$ °C, $P = 1.0$ GPa), the XRD pattern at room temperature showed mainly a cubic phase isostructural with YMn_2D_6 with $a = 6.7172(2)$ Å and an amount of Dy_2O_3 oxide. These results also confirm that the formation of the RMn_2D_6 phase does not depend on the structure of the parent compound and can be obtained equally starting from a C14 or C15 structure, as both structures were present in the parent $DyMn_2$ compound.

The NPD pattern of $DyMn_2D_6$ measured on 3T2 at 300 K can be refined in the same cubic structure as YMn_2D_6 and $ErMn_2D_6$ ($Fm3m$ space group) with a random distribution of Dy and half the Mn atoms on the 8c site and the other half on the 4a site surrounded by six D atoms (table 1 and figure 1). The line widths of the Bragg peaks are quite broad, as observed for YMn_2D_6 and $ErMn_2D_6$, and can be related to the chemical disorder on the 8c site due to the large difference in radius between the R and the Mn atoms.

From 1.5 to 290 K, all the NPD patterns measured on G4.1 were refined in the same cubic structure without significant change in the relative peak intensities (figure 2). No additional line indicating a magnetic long range order was observed from 1.5 to 290 K. However, the difference curve of the G4.1 NPD patterns at 1.5 and 35 K showed a variation in the background

Table 1. Refined atomic positions (x, y, z), occupation number (N), Debye–Waller factor (B), line width parameters (U, V, W, Y), unit cell parameter (a), cell volume (V) and reliability factors (R_I, R_{wp}, R_{exp}, χ^2) for the $ErMn_2D_6$ NPD pattern measured on 3T2 at 300 K. The total occupation number for the Dy and Mn1 atoms on the 8c site was fixed at 1 and the thermal B factors were constrained to be identical for the Dy, Mn1 and Mn2 atoms.

Atoms	Wyckoff position	x	y	z	N	B (Å^2)
Dy	8c	0.25	0.25	0.25	0.500(1)	0.042(5)
Mn1	8c	0.25	0.25	0.25	0.500(1)	0.042(5)
Mn2	4a	0.0	0.0	0.0	1	0.042(5)
D	24e	0.244 98 (1)	0.0	0.0	1	1.035(4)
Line width:	$U = 0.951$	$V = -0.237$	$W = 0.078$	$Y = 0.139$		
Space group: $Fm3m$ (216)						
Lattice parameters: $a = 6.7175(1)$ Å; $V = 303.13(1)$ Å^3						
Agreement factors: $R_I = 6.6\%$ $R_{wp} = 3.6\%$ $R_{exp} = 2.6\%$ $\chi^2 = 1.5$						

Table 2. Magnetic results for RMn_2 and RMn_2D_6 compounds (R = Y, Er, Dy).

Compound	T_C (K)	T_N (K)	M_s (μ_B) (4.2 K)	M_s (μ_B) (5 K)	θ_p (K)	μ_{eff} (μ_B)	χ(μ_B) × 10^6 (290 K)
YMn_2		100				2.7	
YMn_2D_6				0.53	−30	2.0	1.07
$ErMn_2$	25		8.1		0	10.2	7.37
$ErMn_2D_6$	18		5		−11	10.2	7.92
$DyMn_2$	52		8.5		48	10.7	10.33
$DyMn_2D_6$			4.5		−20	10.1	7.32

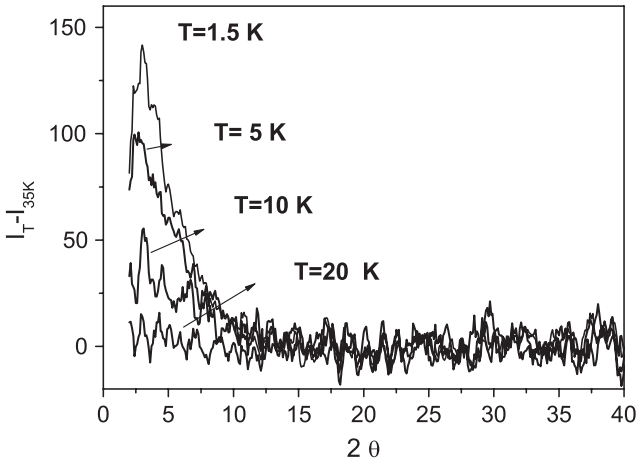

Figure 3. Difference NPD patterns at different temperatures subtracted from $T = 35$ K of $DyMn_2D_6$ measured on G4.1.

intensity below $2\theta = 15°$ (figure 3). This short range order contribution is still visible at 10 K, with a lower intensity, and disappears at 20 K. The background decrease at low angles can be attributed to a short range order ferromagnetic contribution as observed in [6]. A fit of the intensity decrease below 15° assuming noninteracting spherical clusters with a uniform magnetization leads to a spherical radius of 13.5 Å, i.e. close to two nuclear cells. In $ErMn_2D_6$ a broad contribution centred at 30° ($d = 4.75(1)$ Å) was also observed at low temperature and attributed to antiferromagnetic local contribution. This contribution is not clearly observed for $DyMn_2D_6$, but this is possibly masked by the higher signal to noise ratio observed for the NPD patterns of this compound.

3.2. Magnetic measurements

The magnetic properties of the parent $DyMn_2$ compound shows a Curie–Weiss behaviour with $\mu_{eff} = 10.7$ μ_B and a paramagnetic temperature $\theta_p = 48$ K (figure 4). A saturation magnetization of 8.54 μ_B/f.u. is observed at 4.2 K (figure 5) and a Curie temperature of 52 K (table 2). As this compound contains 90% C15 phase and 10% C14, its magnetic properties should be compared to the one published for both C15 and C14 $DyMn_2$ compounds. C15 $DyMn_2$ has a spin-canted ferromagnetic structure with a Dy moment of 8.8 μ_B/Dy and one Mn site in four having a magnetic moment of 1.4 μ_B. A spin reorientation of the Dy moment occurs at 30 K whereas the Curie temperature is estimated at 45 K. It follows a Curie–Weiss behaviour with an effective moment of 10.6 μ_B and a paramagnetic temperature θ_p of 35 K [7]. C14 $DyMn_2$ is ferromagnetic with a Curie temperature of 38 K [8]. The estimated Curie temperature of our compound is slightly higher than that previously published for C15 $DyMn_2$, but it was determined at 5 kOe, whereas the published value was obtained from NPD patterns without applied field.

The saturation magnetization of $DyMn_2D_6$ measured at 4.2 K and extrapolated from 20 T to zero field is $M_S = 4.5$ μ_B (figure 5). Its reverse susceptibility χ^{-1} follows a Curie–Weiss law, parallel to that of $DyMn_2$ with a Curie constant of 12.8 emu mol^{-1} leading to an effective moment $\mu_{eff} = 10.1$ μ_B and a paramagnetic temperature θ_p of −20 K (figure 4). The main effect is therefore a shift of θ_p from a positive value in the intermetallic toward a negative value for the deuteride, showing the existence of negative interactions.

These results are consistent with those observed previously for $ErMn_2D_6$ (table 2) [9]. The saturation magnetization is about half that of the parent compound and θ_p is negative.

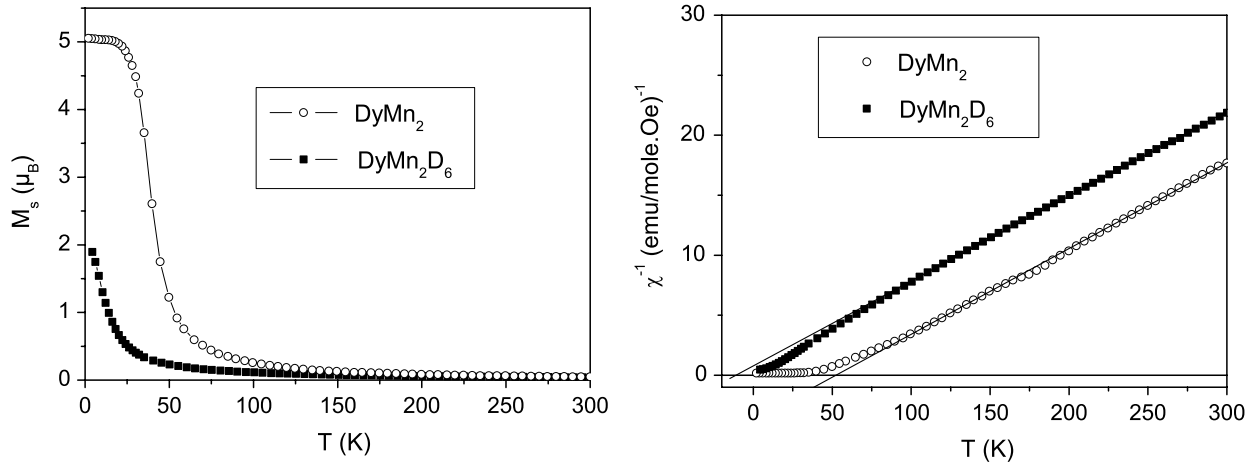

Figure 4. Magnetization and reverse susceptibility of $DyMn_2$ and $DyMn_2D_6$ ($B = 5$ kOe).

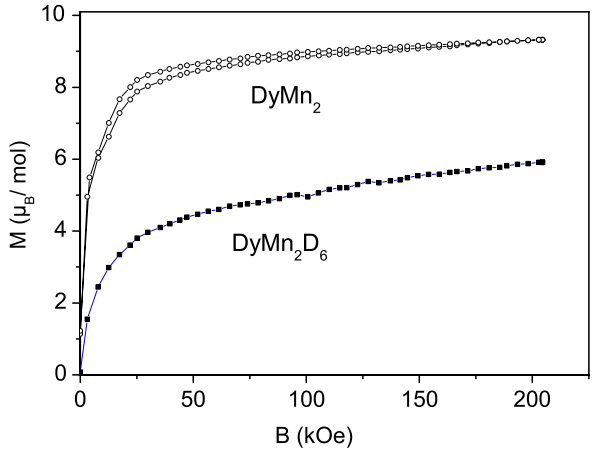

Figure 5. Magnetization of $DyMn_2$ and $DyMn_2D_6$ at 4.2 K.

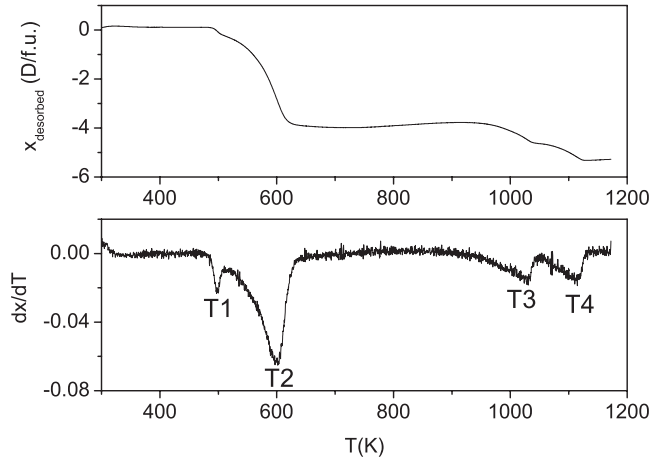

Figure 6. Relative loss of mass and signal derivative of the TGA measurement on $DyMn_2D_6$.

This means that both ferro- and antiferromagnetic R–R interactions should coexist at short range order due to the statistically random distribution of Dy and Mn atoms on the same crystallographic 8c site.

3.3. Thermal stability

The TGA signal of $DyMn_2D_6$, corrected from the Dy_2O_3 contribution, indicates a loss of mass of nearly 2% between 460 and 710 K, corresponding to a total D desorption of 4 D/f.u. (figure 6). The derivative signal shows two peaks with maxima at respectively $T1 = 500$ and $T2 = 600$ K. Subsequent deuterium desorption was observed by TGA, with two peaks centred at 1028 and 1114 K in the derivative signal and an additional weight loss of 1.32 D/f.u. These results are very close to those obtained on $ErMn_2D_6$ [9]. XRD measurement after TGA treatment up to 723 K shows that the compound has decomposed into DyD_2 and Mn. The lines are very broad, indicating rather small particles. The analysis of the line width, using a classical Sherrer method, leads to an average crystallite size of 5(1) nm for DyD_2 and 6(2) nm for Mn. Larger crystal strains are observed for DyD_2 ($\delta d/d = 6.9\%$) than for Mn ($\delta d/d = 1.9\%$). This can also indicate a distribution of deuterium content in the dysprosium deuteride particles. The first loss of mass of 4 D/f.u. therefore corresponds to the following decomposition:

$$DyMn_2D_6 \rightarrow 2Mn + DyD_2 + 2D_2.$$

The desorption peaks at $T3 = 1028$ and $T4 = 1114$ K should be related to a further deuterium desorption of DyD_2 followed by a recombination with Mn. The analysis of the XRD pattern after heating at 1173 K show a mixture of C15 $DyMn_2$ ($a = 7.599$ Å), C14 $DyMn_2$ ($a = 5.355$ Å, $c = 8.7712$ Å), Dy_6Mn_{23} ($a = 12.367$ Å) and $Dy_6Mn_{23}D_x$ ($a = 12.482$ Å). A little unreacted Dy should also be present. The material also contains Dy_2O_3, which was already present in the starting material, but it is possible that a further fraction of Dy has been oxidized at high temperature preventing a full recombination into $DyMn_2$ and explaining the presence of Dy_6Mn_{23}.

Table 3. Cell parameters, experimental and calculated R–Mn interatomic distances in RMn_2D_6 compounds.

Compound	a (Å)	d_{R-Mn} (8c site)	R metallic radius (Å)[a]	$r_R + r_{Mn}$
YMn_2D_6	6.7090(2)	2.9050	1.8012	3.1512
$GdMn_2D_6$	6.7516(2)	2.9240	1.8013	3.1513
$DyMn_2D_6$	6.7172(2)	2.9090	1.7740	3.1240
$HoMn_2D_6$	6.6800(2)	2.8930	1.7661	3.1161
$ErMn_2D_6$	6.6797(2)	2.8920	1.7566	3.1066

[a] Beaudry and Gschneidner, table 2.13 [14]. The metallic radius for Mn is 1.35 Å.

4. Discussion

The structural results obtained on $DyMn_2D_6$ are fully consistent with those obtained previously for YMn_2D_6 and $ErMn_2D_6$, leading to the same crystal structure independently of the C15 or C14 structure of the parent compound. The cubic cell parameter of $DyMn_2D_6$ is slightly larger than that of YMn_2D_6, $HoMn_2D_6$ [10] and $ErMn_2D_6$ and smaller than that of $GdMn_2D_6$ (table 3). This difference between the cell parameters reflects the contraction of the R radii as the atomic number increases. In table 3 the average distances calculated between two neighbouring atoms on the 8c site are compared with the sum of the metallic R and Mn atoms taken from the literature. The interatomic distances are shorter than the sum of the metallic radii and depend of the nature of the R atom. First we should recall that there is a random distribution of R and Mn atoms, and therefore locally we should have a distance distribution between R–R, R–Mn and Mn–Mn pairs of atoms. Then the bonding between the atoms is probably not fully metallic. This is supported by the intermediate position of the cell parameter of YMn_2D_6 between $HoMn_2D_6$ and $DyMn_2D_6$ whereas that of C15 YMn_2 ($a = 7.6795$ Å) is located between $GdMn_2$ ($a = 7.7455$ Å) and $TbMn_2$ ($a = 7.6483$ Å). These results are consistent with those of Siekierski [11] which showed that the relative position of the Y radius compared to other rare earths is related to the type of bonding, and is shifted towards heavier rare earth as the electronegativity of the neighbouring atoms increases. In the case of $Y_{1-x}R_xFe_2H_{4.5}$ compounds, Leblond *et al* [12] have observed that the position of the Y compound is shifted from a value between that of Gd and Tb for the intermetallic compound towards a value between Tb and Er for the corresponding hydride.

Concerning the magnetic properties, as for the other RMn_2D_6 compounds the NPD studies do not show any long range magnetic order down to 1.5 K. Like $ErMn_2D_6$, the saturation magnetization at 4.2 K is almost half that of the parent compound [9]; a negative paramagnetic temperature is extrapolated from the linear part of the magnetization, indicating antiferromagnetic interactions between the R atoms. The NPD analysis reveals the existence of a short range ferromagnetic contribution at low angles and below 15 K. The bump attributed to antiferromagnetic short range order is not clearly visible in the difference patterns for the Dy compound, but the signal to noise ratio is quite low. According to the 18e rules, which apply for isostructural complexes like Mg_2FeH_6, $DyMn_2D_6$ can be expressed as $(Dy^{III}Mn^{II})^{5+}(Mn^{I}D_6)^{5-}$, as already proposed for YMn_2D_6 and $ErMn_2D_6$. However, x-ray absorption measurements on YMn_2D_6 did not show a significant shift of the positions of the Mn-K and Mn-$L_{2,3}$ edges compared to those of YMn_2 and interstitial YMn_2D_x deuterides ($x \leqslant 4.5$) [3]. Therefore further investigations are still needed to solve the electronic structure of this series of RMn_2D_6 compounds.

A remarkable similarity in the thermal desorption behaviour of $ErMn_2D_6$ and $DyMn_2D_6$ is also observed, showing that these compounds decompose around 600 K desorbing about 4 D/f.u. The same type of stability is observed when these compounds are submitted to an applied pressure up to 35 GPa [10]. The compounds remain cubic and their cell volume decreases continuously versus pressure for RMn_2D_6 compounds with R = Y, Dy, Ho and Er. The bulk modulus refined by applying the equation of state to the $V = f(P)$ curves is between 68 and 84 GPa depending of the R element. The study of interstitial YMn_2H_x hydride with 3.4 H/f.u. $\leqslant x \leqslant$ 4.5 H/f.u. showed a change of slope around 8 GPa and a spinodal decomposition occurred for $x \leqslant 2$ [13].

The formation of such RMn_2D_6 phases starting from RMn_2 intermetallics is still under investigation. It is most probable that the interstitial $RMn_2H_{4.5}$ is a precursor of the RMn_2D_6 phase, as in this compound some Mn atoms are surrounded by five D atoms. However, *in situ* neutron diffraction under high hydrogen pressure will be very interesting to confirm this assumption and determine whether an intermediate and unstable phase might be formed at high pressure.

5. Conclusions

The cubic crystal structure of $DyMn_2D_6$ is in agreement with those obtained previously for other RMn_2D_6 compounds with a disordered substitution of Dy and Mn atoms on the same crystallographic site and a complete reorganization of the atomic position compared to that of C14 and C15 parent compounds. The study of the magnetic properties indicates, similar to $ErMn_2D_6$, only a local magnetic order at low temperature with both ferro- and antiferromagnetic interaction between Dy atoms. This result is consistent with the chemical disorder observed on the 8c site. Like the other RMn_2D_6 compounds, this compound is more stable than the interstitial hydrides with lower D content. It first decomposes transforming into Dy deuteride and Mn around 600 K and then the desorption of DyD_2 leads to a recombination of Dy with Mn atoms at 1028 and 1114 K to form intermetallic $DyMn_2$ and Dy_6Mn_{23} compounds.

Acknowledgments

We are grateful to V Lalanne for the synthesis of $DyMn_2$ and E Leroy for the EPMA analysis.

References

[1] Paul-Boncour V, Filipek S M, Marchuk I, André G, Bourée F, Wiesinger G and Percheron-Guégan A 2003 *J. Phys.: Condens. Matter* **15** 4349

[2] Paul-Boncour V, Filipek S M, Percheron-Guégan A, Marchuk I and Pielaszek J 2001 *J. Alloys Compounds* **317/318** 83
[3] Wang C-Y, Paul-Boncour V, Liu R-S, Percheron-Guégan A, Dorogova M, Marchuk I, Hirata T, Filipek S M, Sheu H-S, Jang L-Y, Chen J-M and Yang H-D 2004 *Solid State Commun.* **130** 815
[4] Paul-Boncour V, Filipek S M, Dorogova M, Bourée F, André G, Marchuk I, Percheron-Guégan A and Liu R S 2005 *J. Solid State Chem.* **178** 356
[5] Rodríguez-Carvajal J 1990 *Proc. Congr. Int. Union of Crystallography (Toulouse)* p 127
[6] Hodges J A, Bonville P, Forget A, Yaouanc A, Dalmas de Reotier P, Andre G, Rams M, Krolas K, Ritter C, Gubbens P C M, Kaiser C T, King P J C and Baines C 2002 *Phys. Rev. Lett.* **88** 077204
[7] Ritter C, Kilcoyne S H and Cywinski R R 1991 *J. Phys.: Condens. Matter* **3** 727
[8] Inoue K, Nakamura Y, Tsvyashchenko A V and Fomicheva L 1995 *J. Magn. Magn. Mater.* **140–144** 797
[9] Paul-Boncour V, Filipek S M, André G, Bourée F, Guillot M, Wierzbicki R, Marchuk I, Liu R S, Villeroy B, Percheron-Guégan A, Yang H-D and Pin S C 2006 *J. Phys.: Condens. Matter* **18** 6409
[10] Filipek S M, Sugiura H, Paul-Boncour V, Wierzbicki R, Liu R S and Bagkar N 2008 *J. Phys. Conf. Ser.* **121** 022001
[11] Siekierski S 1981 *J. Solid State Chem.* **37** 279
[12] Leblond T, Paul-Boncour V and Percheron-Guégan A 2007 *J. Alloys Compounds* **446/447** 419
[13] Sugiura H, Paul-Boncour V, Percheron-Guégan A, Marchuk I, Hirata T, Filipek S M and Dorogova M 2004 *J. Alloys Compounds* **367** 230
[14] Beaudry B J and Gschneidner J K A 1978 Preparation and basic properties of the rare earth metals *Handbook on the Physics and Chemistry of Rare Earths* vol 1, ed K A Gschneidner Jr and J L Eyring (Amsterdam: North-Holland) p 173